https://doi.org/10.5194/acp-2022-586
Preprint. Discussion started: 5 September 2022

Atmospheric Chemistry and Physics Discussions

Characteristics and degradation of organic aerosols from cooking sources based on hourly observation of organic molecular markers in urban environment

Rui Li [a, b#], Kun Zhang [a, b#], Qing Li [a, b], Liumei Yang [a, b], Shunyao Wang [a, b], Zhiqiang Liu [a, b, c], Xiaojuan Zhang [a, b, c], Hui Chen [a, b], Yanan Yi [a, b], Jialiang Feng [a, b], Qiongqiong Wang [d], Ling Huang [a, b], Wu Wang [a, b], Yangjun Wang [a, b], Jian Zhen Yu [d, e], Li Li [a, b*]

[a] School of Environmental and Chemical Engineering, Shanghai University, Shanghai, China
[b] Key Laboratory of Organic Compound Pollution Control Engineering (MOE), Shanghai University, Shanghai, China
[c] Jiangsu Changhuan Environment Technology Co., Ltd., Changzhou, Jiangsu, China
[d] Department of Chemistry, Hong Kong University of Science & Technology, Hong Kong, China
[e] Division of Environment & Sustainability, Hong Kong University of Science & Technology, Hong Kong, China

# These two authors contributed equally to this work.

** Correspondence: Li Li (Lily@shu.edu.cn)*

Abstract

Molecular markers in organic aerosol (OA) provide specific source information of $PM_{2.5}$, and the contribution of cooking organic aerosols to OA is significant, especially in urban environments. However, the low time resolution of offline measurements limits the effectiveness in interpreting the tracer data, the diurnal variation of cooking emission and the oxidation process. In this study, we used on-line thermal desorption aerosol gas chromatography mass spectrometry (TAG) to measure organic molecular markers in fine particulate matter ($PM_{2.5}$) at an urban site in Changzhou, China. The concentrations of saturated fatty acids (SFA), unsaturated fatty acids (uFAs), and oxidative decomposition products of unsaturated fatty acids (ODPs) were measured every two hours to investigate the temporal variations and the oxidative decomposition characteristics of uFAs in urban environment. The average concentration of total fatty acids (TFAs, sum of sFAs and uFAs) was measured to be 105.70± 230.28 ng/m^3. The average concentration of TFAs in polluted period ($PM_{2.5}$ > 35 μg/m^3) was 147.06 ng/m^3, which was 4.2 times higher than that in clean period ($PM_{2.5}$ < 35 μg/m^3), higher

https://doi.org/10.5194/acp-2022-586
Preprint. Discussion started: 5 September 2022


Atmospheric Chemistry and Physics Discussions

than the enhancement of $PM_{2.5}$ (2.2 times) and OC (2.0 times) concentrations comparing polluted period to clean period. The mean concentration of cooking aerosol in the polluted period (3.63 μg/m^3) was about 3.9 times higher than that in the clean period (0.90 μg/m^3), which was similar to the trend of fatty acid. During the rising period of $PM_{2.5}$, TFAs concentration tends to reach the peak earlier than $PM_{2.5}$. Fatty acids showed a clear diurnal variation. Linoleic acid /Palmitic acid and Oleic acid /Palmitic acid ratios were significantly higher at dinning time, and closer to the source profile. By performing backward trajectory clustering analysis, under the influence of short-distance air masses from surrounding areas, the concentrations of TFAs and $PM_{2.5}$ were relatively high; while under the influence of air masses from easterly coastal areas, the oxidation degree of unsaturated fatty acids emitted from local culinary sources were higher. The effective rate constants (k_O) for the oxidative degradation of oleic acid were estimated to be 0.12-0.41 h^{-1}, which were lower than k_L (the estimated effective rate constants of linoleic acid, 0.25-0.50 h^{-1}). Both k_O and k_L showed a significant positive correlation with O_3, indicating that O_3 was the main night-time oxidants for uFAs in the Changzhou City. Using fatty acids as tracers, cooking was estimated to contribute an average of 4.8% to $PM_{2.5}$ concentrations, rising to 6.1% at dinner time; while the contribution to total OC is more than double the contribution to $PM_{2.5}$. This study investigates the variation of the concentrations and oxidative degradation of fatty acids and corresponding oxidation products in ambient air, which can be a guide for the refinement of aerosol source apportionment, and provide scientific support for the development of cooking source control policies.

1. Introduction

Organic aerosol (OA) is an important component of fine particulate matter ($PM_{2.5}$), accounting for 20-90% of the total $PM_{2.5}$ mass (Kanakidou et al., 2005). Among different OA sources, restaurant fumes are relatively important (Huang et al., 2021). The contribution of cooking organic aerosols (COA) to OA is significant, especially in urban environments, where COA can contribute 11%-34% to total OC and 3%-9% to $PM_{2.5}$ mass concentration, even higher than traffic-related hydrocarbon-based OA (Huang et al., 2021; Li et al., 2020). The presence of carcinogenic mutagens in restaurant fumes contains chemicals that can be harmful to human immune function (Huang et al., 2020). According to the 2018 global cancer statistics, lung cancer accounts for 24.1% of all cancer deaths in China and is the most common cause of cancer-related deaths in China. The risk of cancer is associated with cooking events (Zhang et al., 2017). In previous studies on the molecular tracers of cooking source based on filter membrane sampling, the time resolution usually varies from one day to several days, which cannot accurately capture the diurnal variations of pollutants emitted by the cooking source (Li et al., 2021). The aerosol gas chromatography−mass spectrometry (TAG) enables possible monitoring of

https://doi.org/10.5194/acp-2022-586
Preprint. Discussion started: 5 September 2022


Atmospheric Chemistry and Physics Discussions

organic molecular markers (Wang et al., 2020). By clarifying the characteristics of cooking emissions, quantifying the concentrations of pollutants emitted from cooking and its contribution to OA, can effectively reduce their impact on environmental pollution and human health, and help the government to formulate more scientific and reasonable pollution prevention and control policies.

Processes such as emission rate, atmospheric dilution, and photochemical oxidation can affect aerosol composition measured at receptor sites (Fortenberry et al., 2019; Yee et al., 2018). Particulate organic matter can undergo heterogeneous oxidation by ozone, OH and NO_3 radicals (Wang et al., 2020). When using organic tracer data from filter analysis, variations in concentration due to degradation or secondary production were reported (Ringuet et al., 2012). These degradation and generation processes in the atmosphere are therefore worthy of our attention when using organic markers as source tracers. The mechanism and kinetics of ozonolysis of oleic acid and linoleic acid in the presence of oxidants such as NO_3, O_3 and OH radicals have been extensively studied (Vesna et al., 2009; Zahardis and Petrucci, 2007; Ziemann, 2005). The aging of POA markers under atmospheric conditions is still far from being properly understood with few field observations performed in this topic compared to laboratory studies, for which highly time-resolved observations would help to fill this gap (Bertrand et al., 2018a; Bertrand et al., 2018b).

Cooking is an important source contributor to $PM_{2.5}$, especially in urban environments. Cooking sources have recently received increasing attention, but they are largely an uncontrolled source of $PM_{2.5}$. Saturated fatty acids (sFAs) and unsaturated fatty acids (uFAs), such as palmitic, stearic, and oleic acids, are known molecular markers for culinary emissions, which are released primarily during cooking activities from the hydrolysis and thermal oxidation of cooking oils. Fatty acids and their derivatives are often used in the receptor source apportionment of $PM_{2.5}$. It has been found that nonanoic acid, X9-oxononononanoic acid and azelaic acid are the main atmospheric oxidation products of oleic acid, while unsaturated fatty acids such as oleic and linoleic acids also react with other atmospheric oxidants, such as OH (Nah et al., 2014; Wang et al., 2020).

In this study, TAG was employed at an urban site in Changzhou, China, to investigate the variation of atmospheric cooking-related fatty acids (FAs) with hourly resolution data (Ren et al., 2019). The aim of this study is to identify the contribution of culinary emissions to ambient $PM_{2.5}$ with hourly organic molecules data and to investigate the oxidative decomposition reactions of cooking-related FAs in an urban area. Results of this study could provide valid basis and insights for the refinement of $PM_{2.5}$ source apportionment as well as atmospheric modelling.

https://doi.org/10.5194/acp-2022-586
Preprint. Discussion started: 5 September 2022

Atmospheric Chemistry and Physics Discussions

2. Methodology

2.1 Online measurements

Gaseous pollutants, $PM_{2.5}$ and its main chemical constituents as well as organic markers were measured online at the Changzhou Environmental Monitoring Center of Jiangsu Province (CEMC) (31.76N, 119.96E) during January-March 2021, which is a representative urban site (Fig. 1) Detailed information on instruments can be found in Text S1 of the Supporting Information. The meteorological parameters and gas pollutant data were obtained from CEMC observations and publicly available datasets from the China Meteorological Data Network (available at http://data.cma.cn, last access: Aug 16, 2022).

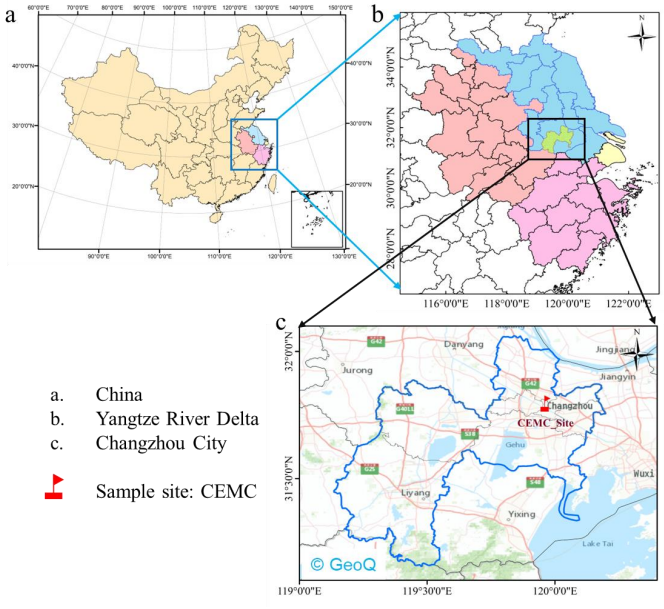

Figure 1. Locations of the sampling site in Changzhou, China.

Quantification of hourly speciated organic markers were achieved using TAG. The operation details and data quality have been described in our previous work (Wang et al., 2020; Zhang et al., 2021). Ambient air was drawn through a $PM_{2.5}$ cyclone, then the sampled air was collected after passing through a carbon denuder to remove the gas phase so that only particles were collected. The organics were then desorbed and transferred from the collection matrix to the GC column, with in-situ derivatization of the polar organics under a variable stream of saturated helium with derivatization agent (N-methyl-N-(trimethylsilyl) trifluoroacetamide). After GC separation the target organics entered the MS chamber for analysis. With the current TAG instrumental set-up, samples were collected every even hour, thus yielding a

https://doi.org/10.5194/acp-2022-586
Preprint. Discussion started: 5 September 2022

Atmospheric Chemistry and Physics Discussions

maximum of 12 hourly samples per day. The post-sampling steps, including in-situ derivatization, thermal desorption, and GC/MS analysis, took ~1.5 h, and the next sampling started concurrently with the GC/MS analysis step (An et al., 2020).

The summary of target organic molecular markers and internal standards (IS) are shown in Table 1. Identification of compounds was performed by comparing retention times and mass spectra with those of authentic standards (Vesna et al., 2009; Wang et al., 2020). Calibration curves were established by internal standard method. The correlation coefficients of the calibration curves range from 0.88-1.00. For compounds without authentic standards and for compounds whose authentic standards are not included in the current standard mixture, their identification is performed by comparing their mass spectra with the National Institute of Standards and Technology (NIST) libraries. Azelaic acid was identified and quantified by using authentic standards. Nonanoic acid and X9-oxononanoic acid were identified by comparison with mass spectra in the NIST library and by referring to Ziemann (2005), Pleik et al. (2016) and Wang et al. (2020). Ozone oxidation of oleic acid yields C_9 aldehydes and acids including nonanal, azelaic acid, nonanoic acid, and X9-oxononanoic acid. Since nonanal could also be primary in the gas phase, it is thus not discussed in this paper. The library of the NIST was identified and quantified using the alternative standards specified in Table 1.

Table 1. Statistics of hourly concentrations of organics associated with cooking emissions measured by TAG during the campaign.

Compounds	Average	Stdev	Min	Max	Quantification IS
Myristic acid [a]	0.69	1.33	0.03	10.14	Palmitic acid-d_{31}
Palmitic acid	38.77	84.14	1.45	670.12	Palmitic acid-d_{31}
Stearic acid	26.51	50.58	1.81	341.65	Palmitic acid-d_{31}
Oleic acid	32.15	81.34	0.96	723.95	Stearic acid-d_{35}
Linoleic acid [b]	7.80	28.32	0.09	326.50	Stearic acid-d_{35}
Nonanoic acid [c]	1.19	1.32	BD [d]	7.94	Adipic acid-d_{10}
X9-oxononanoic acid [c]	3.91	4.73	0.19	17.18	Adipic acid-d_{10}
Azelaic acid	9.15	32.99	BD	309.64	Adipic acid-d_{10}

a, Quantified using palmitic acid as the surrogate; b, Quantified using oleic acid as the surrogate; c, Quantified using azelaic acid as the surrogate; d, Below detection limit.

2.2 Backward trajectory analysis

Backward trajectory analysis is a useful tool in identifying the influence of air masses on the chemical composition of $PM_{2.5}$ (Wang et al., 2017). Backward trajectories of 36-h duration arriving at an altitude of 100 m above ground level (AGL) over the CEMC site were calculated deploying the 0.5° Global Data Assimilation System (GDAS) meteorological data (https://www.ready.noaa.gov/archives.php, last access: Aug 16, 2022). The trajectories were then classified into different clusters according to the geographical origins and movement of the trajectories using the TrajStat model (Li et al., 2020).

https://doi.org/10.5194/acp-2022-586
Preprint. Discussion started: 5 September 2022

Atmospheric Chemistry and Physics Discussions

2.3 Relative rate constant analysis

Ambient concentrations of species are influenced by its emissions, atmospheric dilution/compaction, chemical loss/production, and wet/dry deposition. As the target sFAs and uFAs in urban environments are predominately primary in their source origin, the chemical production rate could be assumed to be negligible. Donahue et al. (2005) formulated the relative rate expression for heterogeneous oxidation reactions of multicomponent OA (Huff et al., 2007). The specific expression as applied to the ambient measurements of uFAs is derived, as given in Equation (Eq 1) and Equation (Eq 2) (Wang and Yu, 2021).

$$\frac{C_i}{C_s} = A \times e^{-kt} \quad (1)$$

$$k \approx k_{r_i} \times C_{OX} \quad (2)$$

C_i and C_s are the particle-phase concentration of species i and sFAs, respectively. Among the quantified sFA and uFA cooking markers, palmitic acid was selected as the reference molecule for normalization. Using the concentration ratio eliminates the interference from atmospheric dilution and deposition. Fitting the ambient C_i/C_s data versus t with an exponential function provides an estimate for k, the effective pseudo-first order decay rate (h^{-1}). k_{ri} is the second-order reaction rate constant of species i against an oxidant. C_{OX} is the average oxidant concentration in the aerosol.

2.4 Source apportionment based on PMF

Positive Matrix Factorization (PMF) is a bilinear factor analysis method, which is widely used to identify pollution sources and quantify their contributions to the ambient air pollutants at receptor sites, with an assumption of mass conservation between emission sources and receptors (Amato et al., 2009; Lee et al., 2008). In this study, the United States Environmental Protection Agency (USEPA) PMF version 5.0 (Norris et al., 2014) was applied to perform the analysis. PMF decomposes the measured data matrix, X_{ij}, into a factor profile matrix, f_{kj}, and a factor contribution matrix, g_{ik}, (Eq 3):

$$x_{ij} = \sum_{k=1}^{p} g_{ik} f_{kj} + e_{ij} \quad (3)$$

$$Q = \sum_{i=1}^{n} \sum_{j=1}^{m} (e_{ij}/u_{ij})^2 \quad (4)$$

where X_{ij} is the measured ambient concentration of target pollutants; g_{ik} is the source contribution of the k_{th} factor to the i_{th} sample, and f_{kj} is the factor profile of the j_{th} specie in the k_{th} factor; e_{ij} is the residual concentration for each data point. PMF seeks a solution that minimizes an object function Q (Eq 4), with the uncertainties of each observation (u_{ij}) provided by the user.

The uncertainty of each data point was calculated according to Eq 5:

https://doi.org/10.5194/acp-2022-586
Preprint. Discussion started: 5 September 2022

Atmospheric Chemistry and Physics Discussions

$$u_{ij} = \sqrt{(x_{ij} \times EF)^2 + (\frac{1}{2} \times MDL)^2} \quad (5)$$

where MDL is the method detection limit and *EF* is the error fraction determined by the user and associated with the measurement uncertainties. The concentration data below MDL was replaced by 0.5 of the MDL, and the corresponding uncertainty u_{ij} was calculated by five-sixths of the MDL. Missing values were replaced by the median value of the species, and its u_{ij} was assigned as four times of the median value (Norris et al., 2014).

3. Results and discussion

The time series of hourly data of meteorological parameters, gaseous pollutants (including O_3 and NO_2), $PM_{2.5}$, water soluble ions (WSII, including sulfate, nitrate, ammonium, and other ions), carbon components (Organic carbon, OC; Elemental carbon, EC) during the monitoring period (January 10-14, February 9-15 and March 11-16, 2021) are shown in Fig.2. During the campaign, the average temperature (T), relative humidity (RH) and wind speed (WS) was 10.9±4.5 ℃, 55.3±18.2% and 1.2±0.5 m/s, respectively. The average concentrations of gas pollutants, $PM_{2.5}$, WSII and OC/EC are listed in Table S1. The average concentrations of NO_2, O_3 and $PM_{2.5}$ were 42.85±25.89, 51.53±29.62 and 50.07±26.54 μg/m^3, respectively. Additionally, the average OC and EC concentrations were 6.57±4.63 and 2.12±2.04 μg/m^3 respectively, with the contribution of OC to $PM_{2.5}$ ranging from 4.7% to 26.8% (13.2% as average).

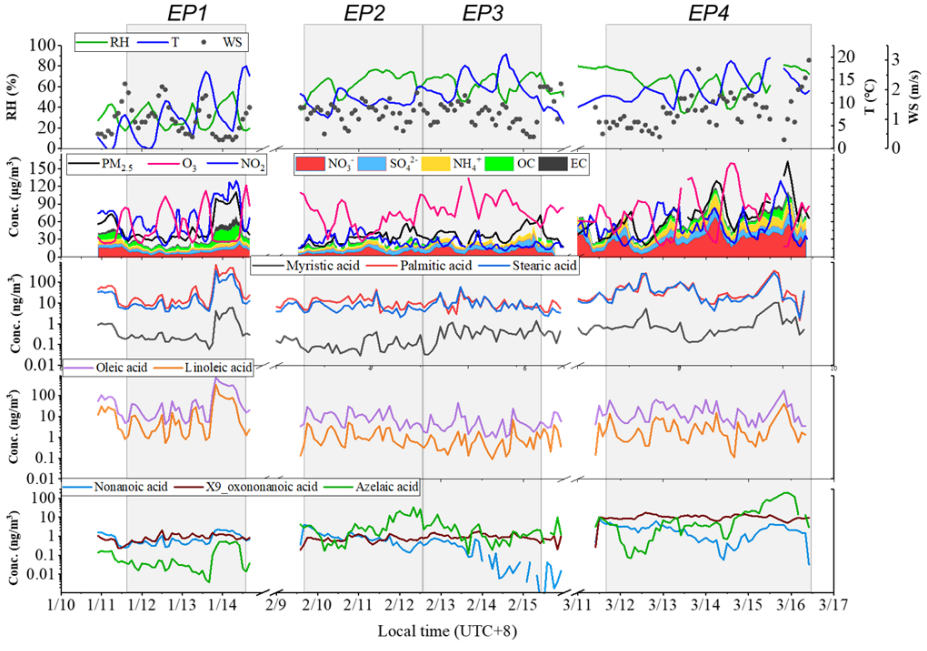

Figure 2. Time series of pollutants concentration and meteorological parameters

https://doi.org/10.5194/acp-2022-586
Preprint. Discussion started: 5 September 2022

Atmospheric Chemistry and Physics Discussions

3.1 Characteristics of cooking-derived organic molecular markers

The concentration of TFAs (sum of the concentrations of the five fatty acids, including myristic acid, palmitic acid, stearic acid, oleic acid and linoleic acid) was (105.70±230.28) ng/m^3, ranging between 8.30—2066.30 ng/m^3, which is close to the concentrations at the urban site in Shanghai (105 ng/m^3) (Li et al., 2020; Wang et al., 2020). The average percentage of TFAs in OC was 1.3% and the maximum was 8.7% (The concentration of $PM_{2.5}$ at the corresponding time was 99 μg/m^3), which was 6.6 times higher than the average. It revealed that the composition of $PM_{2.5}$ could dramatically change, especially during the dinner time. The mean concentration of TFAs at dinner time was 160.71 ng/m^3, and the contribution of FAs to $PM_{2.5}$ and OC mass concentration was 2.4‰ and 1.7%, respectively, which were 1.5 and 1.3 times of the mean during the observation period.

The fatty acids studied here include three most abundant saturated fatty acids (myristic, palmitic and stearic acids) and two unsaturated fatty acids (oleic and linoleic acids). Similar variation and diurnal patterns were found for these five FAs (Fig.2 and Fig.3), confirming their common origin. In addition, compared to FAs, the time series of C_9 acids showed a different diurnal variation, suggesting different production and reaction processes.

Fatty acids showed a clear diurnal variation, with two peaks monitored at around 6:00 and 20:00 local (LST, UTC+8), respectively, especially prominent at the dinner time. In contrast to the previous observations in Shanghai, no peak was observed at the lunchtime. The relatively higher boundary layer during the day, which facilitates the diffusion of pollution and the weaker oxidation of fatty acids emitted at night make the fatty acid concentration peaks more pronounced at dinner time (Wang et al., 2020). In conclusion, the apparent peaks of total fatty acids at the dinner time provide strong evidence for source contribution to air pollution from local cooking emissions.

https://doi.org/10.5194/acp-2022-586
Preprint. Discussion started: 5 September 2022

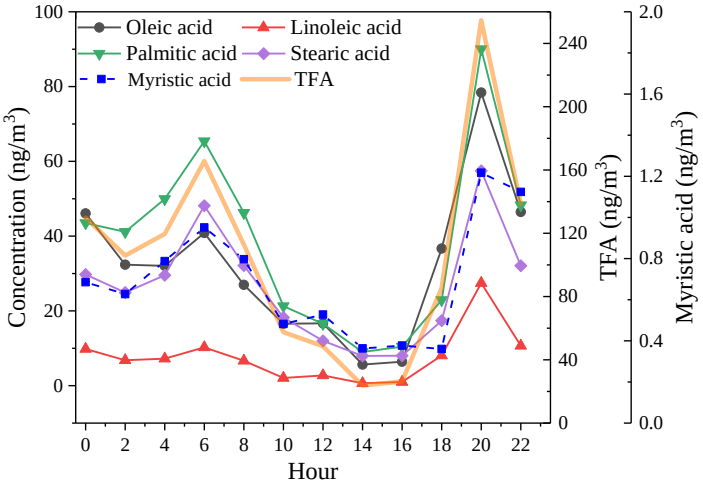

Figure 3. Diurnal variation of five fatty acids and total fatty acids during the observation period.

Information on the changes of specific molecular markers is useful in investigating the aging process of aerosol. The two uFAs (oleic acid and linoleic acid) are more reactive with atmospheric oxidants (OH and O_3, etc.) in the atmosphere due to the presence of C=C bonds compared to saturated fatty acids. Furthermore, the two homologous saturated fatty acids (palmitic and stearic acid) have similar chemical structures, reactivity and volatility, so that their concentration ratios can be assumed to remain constant post-emission. Therefore, the ratio of palmitic to stearic acid should mainly depend on the sources. Fig.4 shows the oleic acid/ palmitic acid (O/P) ratios and linoleic acid/ palmitic acid (L/P) versus palmitic acid to stearic acid (P/S), respectively. The average value of P/S was 1.49±0.49, which was within the range of source profile values measured from different restaurants in China (1.3-8.1) (He et al., 2004; Pei et al., 2016; Schauer et al., 2002; Zhao et al., 2007) and was lower than the ratio of palmitic acid to stearic acid in atmospheric $PM_{2.5}$ in Shanghai (1.9) (Li et al., 2020; Wang et al., 2020). The oleic acid/ palmitic acid ratio (0.87 ± 0.67) was overall in the range of the source profile (0.6-2.8, with an average of 1.43), while the linoleic acid/ palmitic acid ratio of 0.16 ± 0.17 was slightly lower than the source profile values (0.2-3.2, and the average was 1.31) (He et al., 2004; Pei et al., 2016; Schauer et al., 2002; Zhao et al., 2007), indicating that linoleic acid is more easily degraded than oleic acid. The oleic acid / palmitic acid ratio was higher than those measured in Beijing (0.12) (He et al., 2004) from January to October and in Shanghai (0.13) (Li et al., 2020; Wang et al., 2020) during winter.

The diurnal variations of O/P and L/P are also shown in Fig.4. The ratios were significantly higher during dinner time (18:00-20:00) and were closer to the source profile values. Demonstrating that fresh emissions entered into the atmosphere during cooking period, especially dinner time, while unsaturated fatty acids were quickly consumed via

https://doi.org/10.5194/acp-2022-586
Preprint. Discussion started: 5 September 2022

Atmospheric Chemistry and Physics Discussions

reactions with atmospheric oxidants. The ratio of linoleic acid to palmitic acid is consistently lower than what is involved in the source spectrum, which may be influenced by different regions and source characteristics from different types of restaurants, and is also related to the atmospheric oxidation capacity.

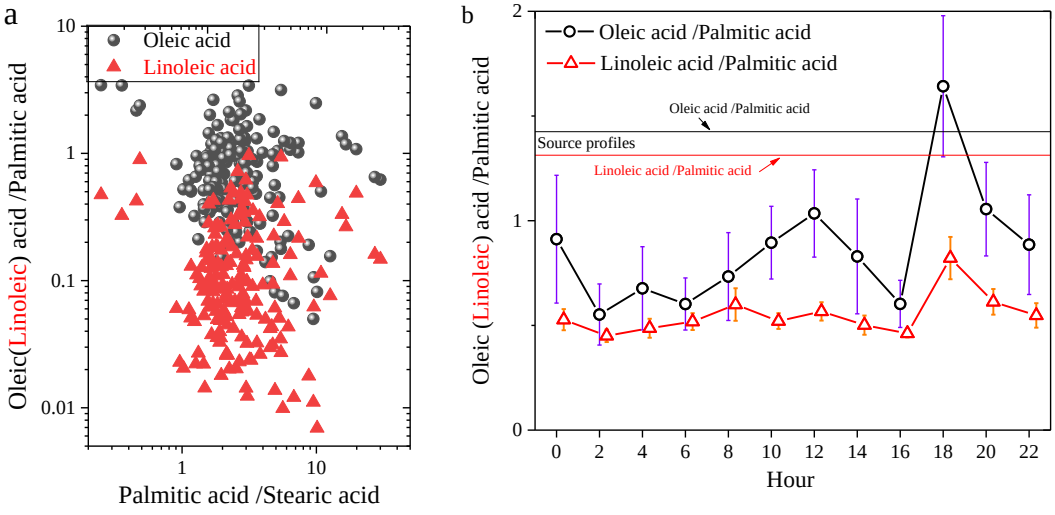

Figure 4. The oleic/ palmitic acid and linoleic/ palmitic acid ratios compared to the palmitic/stearic acid ratio (a); diurnal variation in the ratio of oleic (linoleic) acid to palmitic acid concentration (b).

3.2 Backward trajectory clustering analysis

The best solution for the four clusters was determined based on the variation of the total spatial variance (Fig.5 and Figure S2). Fig.6 shows the four cluster solutions and the mean distribution of meteorological conditions and pollutants in each cluster. Briefly, cluster #1 (CL#1), which represents 15.4% of the sample, comes from the northwest continental region of China and reaches Changzhou before passing Gansu, Shaanxi and Henan provinces, and the lower temperatures and humidity associated with this cluster are consistent with its geographic origin. Cluster #2 (CL#2), which accounts for 35.6% of the total number of trajectories, represents air masses from the northeastern part of the ocean, and the temperature and humidity associated with this cluster are higher than those of CL#1. Cluster 3 (CL#3), contributing 18.6%, travaeling slowly from inland area, is associated with the lowest wind speed observed, with higher temperature and humidity than CL#1 but lower than CL#2. Gluster 4 (CL#4), representing 30.3% of the trajectories, represents the eastern/southeastern oceanic air masses, with the highest observed temperature, humidity and wind speed among all of the air masses. CL#2 and CL#4 have relatively high temperature, humidity and wind speed. CL#3 is associated with the highest NO_2 concentrations, confirming its local air mass origin, and the $PM_{2.5}$ and OC concentrations in this air mass are

https://doi.org/10.5194/acp-2022-586
Preprint. Discussion started: 5 September 2022

Atmospheric Chemistry and Physics Discussions

also the highest compared to all the other air masses.

The concentrations of saturated (unsaturated) fatty acids, unsaturated acids and their oxidation products under each cluster are shown in Fig.5. The total concentrations of sFAs, uFAs and unsaturated fatty acids oxidative decomposition products (ODPs) under the four types of air mass clusters were in the order of CL#3>CL#2>CL#4>CL#1, where the TFAs in CL#1 and CL#3 were larger than the percentages in CL#2 and CL#4. The relative contents of sFAs and uFAs in CL#1 and CL#3 are closer than those in the other two types of air masses, and are closer to the concentration ratio of the species directly emitted from the cooking source (the value of uFAs /sFAs range from 0.8 to 3.2) (He et al., 2004; Pei et al., 2016; Schauer et al., 2002; Zhao et al., 2007), which indicated that the oxidative decomposition of unsaturated fatty acids is less in CL#1 and CL#3. The value of uFAs /sFAs in CL#2 and CL#4 was less than that in CL#1 and CL#3 and less than the ratio in sources. In addition, the proportion of oxidation ODPs in CL#2 and CL#4 is greater than that in CL#1 and CL#3. This phenomenon may be explained by the following two reasons: first, under the influence of transportation, the air masses bring more saturated fatty acids and the air masses are more aged; second, the oxidative decomposition reactivity of unsaturated fatty acids emitted from local restaurant sources is higher and produces more oxidation products when CL#2 and CL#4 air masses are under the influence of CL#4. In addition, the oxidative reaction of unsaturated fatty acids could be influenced by meteorological conditions as well.

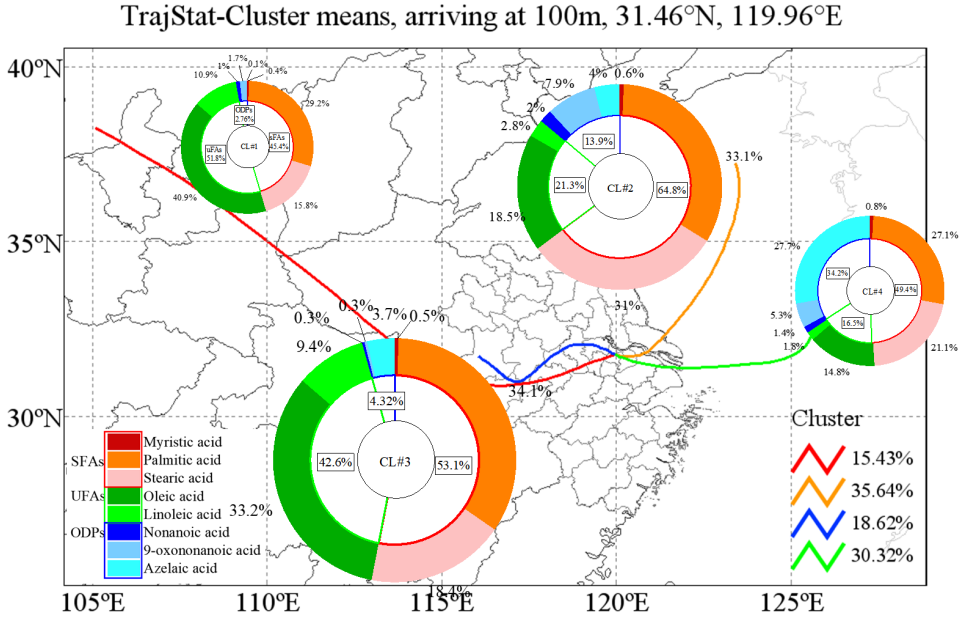

Figure 5. Sources for each air mass during the sampling period. The colored lines in the map show the contribution of each directional air mass source to the total trajectory as resolved by the TrajStat model.

https://doi.org/10.5194/acp-2022-586
Preprint. Discussion started: 5 September 2022

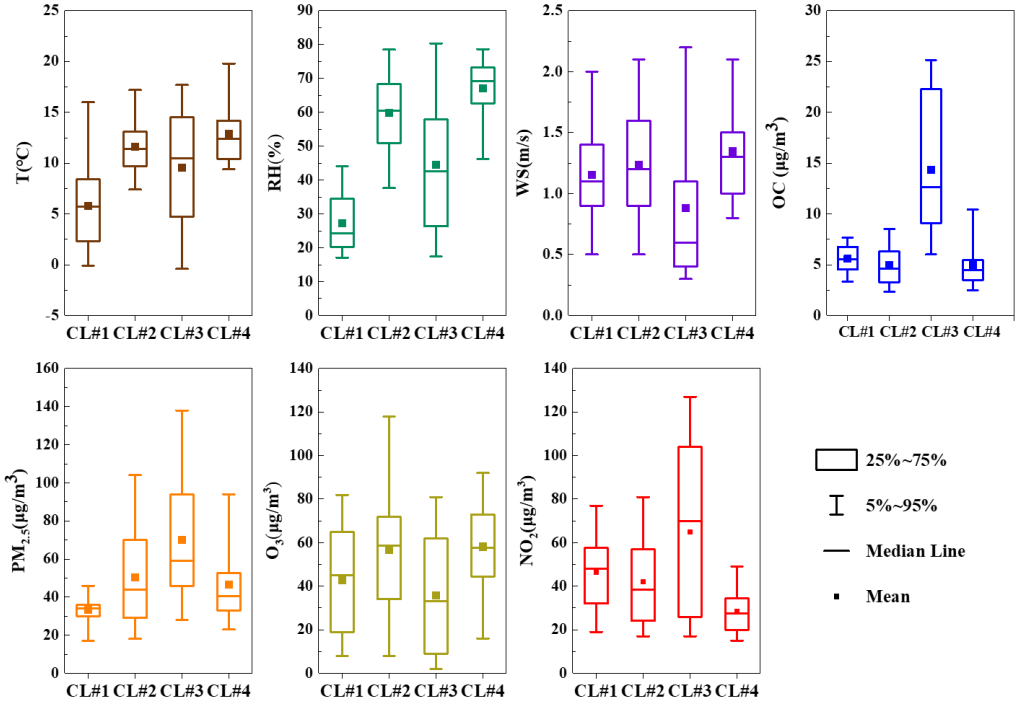

Figure 6. Box plots of meteorological parameters and pollutant concentrations in each cluster (squares and solid lines correspond to the mean and median, respectively; boxes indicate the 25th and 75th percentiles, whiskers are the 5th and 95th percentiles).

3.3 Characteristics of fatty acids in episode periods

We define the "polluted period" as the periods with hourly $PM_{2.5}$ concentrations exceeding 35 μg/m^3, whereas other periods are defined as "clean period". Table 2 shows the mean values of $PM_{2.5}$, OC and TFAs concentrations during the clean ($PM_{2.5}$ <35μg/m^3) and polluted periods. The mean concentration of $PM_{2.5}$ during the polluted period was 62.86 μg/m^3, which was 2.2 times higher than that during the clean period (28.29 μg/m^3). OC and $PM_{2.5}$ were similar, with concentrations during the pollution period being 2.0 times higher than during the clean period. The mean concentration of TFAs in the polluted period was 147.06 ng/m^3, which was 4.2 times higher than that in the clean hour (35.28 ng/m^3). Additionally, the concentrations of sFAs and uFAs in the polluted hour were 4.3 and 4.1 times higher than those at the clean period, respectively.

The concentration of TFAs may be influenced by emissions, accumulation, transport and dispersion of pollutants during the polluted periods (Hou et al., 2006; Schauer et al., 2003). The fatty acid content of 1.95 ng/μg in $PM_{2.5}$ at the polluted period was 2.7 times greater than that of 1.24 ng/μg at the clean period, which was smaller than the variation

https://doi.org/10.5194/acp-2022-586
Preprint. Discussion started: 5 September 2022

Atmospheric Chemistry and Physics Discussions

range of $PM_{2.5}$ and OC concentrations before and after the polluted period. The variation of TFAs in OC was similar to that in $PM_{2.5}$. The change in TFAs/OC was weaker than the change in OC, mainly because cooking has relatively small fluctuations in emissions, while the increase in OC concentration was more significant with simultaneous contributions from other sources (e.g., biomass burning, coal combustion, and vehicle exhaust). Similarly, the mass concentration of $PM_{2.5}$ was driven by emission source significantly.

Table 2. $PM_{2.5}$ concentration, organic carbon fraction and fatty acids concentration during clean and polluted periods.

Species	Clean period	Polluted period	Polluted/clean
$PM_{2.5}$ (μg/m^3)	28.29	62.86	2.2
OC (μg/m^3)	4.05	8.00	2.0
TFAs (ng/m^3)	35.28	147.06	**4.2**
sFAs (ng/m^3)	21.60	92.05	**4.3**
uFAs (ng/m^3)	13.68	55.53	**4.1**
TFAs/$PM_{2.5}$ (ng/μg)	1.24	1.95	1.6
TFAs/OC (ng/μg)	16.84	22.61	1.3

To better analyze the effect of cooking source on $PM_{2.5}$ before and after pollution episode, four episodes (EP) were selected for further analysis (Fig.7). The time period before the $PM_{2.5}$ peak concentration was defined as one episode, and four episodes (EP1-EP4) were observed. Considering that the emission intensity of the cooking source was relatively large at night, in order to avoid dividing an emission process into different days, 16:00 pm to 14:00 of the next day was defined as one day, and EP1-EP3 includes 3 days (D1-D3). In EP1, the value of TFAs/$PM_{2.5}$ increased with the increase of $PM_{2.5}$ concentration. The wind speed of D1-D3 continued to decrease, and affected by the CL#3 air mass, the wind speed in D3 was only 0.58m/s. The lower wind speed was not conducive to the diffusion of pollutants, and the impact of regional transport on observation sites was also reduced, and the concentrations of $PM_{2.5}$ and OC increased cumulatively. As a local source, the contribution of TFAs emitted by cooking source to $PM_{2.5}$ concentration in EP1 increased with increasing $PM_{2.5}$ concentration.

In EP2-EP4, $PM_{2.5}$ reached a peak on D3, however, the concentration contribution from TFAs to $PM_{2.5}$ (TFAs/$PM_{2.5}$) in D3 was smaller than that of D1 and D2. This common conclusion can be attributed to the fact that the air mass transport brings less fatty acids in particulates compared to local emissions, thereby diluting TFAs concentration in $PM_{2.5}$ observed (Guo et al., 2004). Especially in EP2, influenced by air mass CL#2 and CL#4, the wind speed fluctuated little, and the variation trend of TFAs/$PM_{2.5}$ was opposite to that of $PM_{2.5}$ average concentration. In EP2, when the D1-D3 air mass gradually changed from CL#2 to CL#4, the concentration of uFAs oxidation products (ODPs) showed an upward trend and reached the peak of ODPs concentration in D3 (15.43ng/m^3), which was consistent with the conclusion in Fig.5

https://doi.org/10.5194/acp-2022-586
Preprint. Discussion started: 5 September 2022

Atmospheric Chemistry and Physics Discussions

in section 3.2. In EP4, the average concentration of $PM_{2.5}$ in D3-D5 days was greater than 75μg/m^3, resulting in $PM_{2.5}$ pollution, while the relative mass of TFAs in $PM_{2.5}$ was smaller than that of D2, indicating that TFAs were more advanced than $PM_{2.5}$ during the period of particulate pollution reach the peak concentration (Hou et al., 2006). However, the concentration of TFAs during $PM_{2.5}$ pollution (the average concentration of TFAs in D3-D5 of EP4 was 123.63 ng/m^3) was greater than that before the peak of TFAs (the concentration of TFAs in D1 of EP4 was 56.11 ng/m^3). Consistent with the change characteristics of ODPs in EP2, the concentration of ODPs increased when the air mass in EP4 changed from CL#2 to CL#4 of D4 and D5.

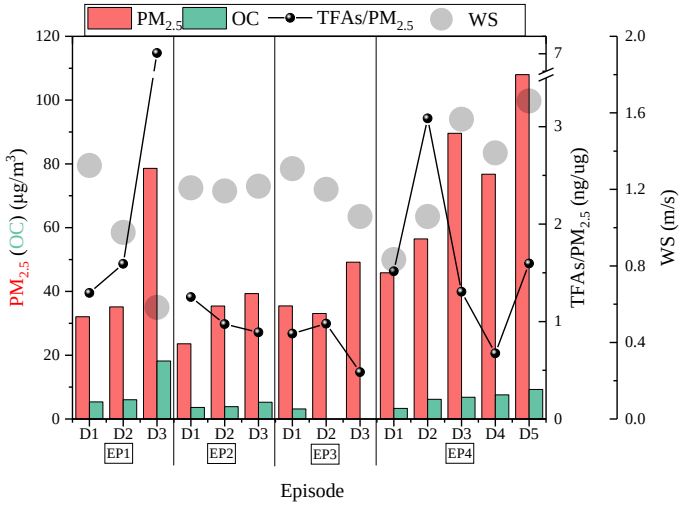

Figure 7. Variation of pollutants concentration and wind speed in different episodes.

3.4 Atmospheric aging of cooking markers

Fig.8(b) to (d) shows the correlation between ODPs /palmitic acid ratio and oleic acid/palmitic acid. Azelaic acid and X9-oxononanoic acid were negatively correlated with oleic acid. The ozone concentration started to rise in the morning (06:00) and peaked in the late afternoon (14:00) (Fig.8(a)). The diurnal trend of oleic acid was opposite to that of ozone. A small peak of azelaic acid concentration was found at around 12:00, which was earlier than that of ozone. At the same time, oxidative decomposition causes the concentration of oleic acid falling significantly until the dinner time when large amounts of fresh emissions enter the atmosphere again. The decreasing rate of oleic acid concentration slowed down around noon, probably because of fresh cooking emission at lunch time, and slower chemical consumption, which eventually led to flat consumption. The diurnal variations of the other two products of ozone decomposition of oleic acid (Nonanoic acid and X9-oxononanoic acid) were similar and both peaked around noon, while the production of

https://doi.org/10.5194/acp-2022-586
Preprint. Discussion started: 5 September 2022

Atmospheric Chemistry and Physics Discussions

X9-oxononanoic acid and azelaic acid are in competition (Thornberry and Abbatt, 2004). However, the concentration of X9-oxononanoic acid was significantly higher than that of nonanoic acid, which may be due to the following reasons: (1) X9-oxononanoic acid can be produced by two pathways, while nonanoic acid generation can only be produced through one of the pathways competing with nonanal, and the molarity generated from the ozonolysis of oleic acid is smaller than that of X9-oxononanoic acid (Gross et al., 2009); (2) due to the high volatility of nonanoic acid, its concentration in the particle phase is much lower, and only a small portion of nonanoic acid TAG present in PM is detected (Wang and Yu, 2021).

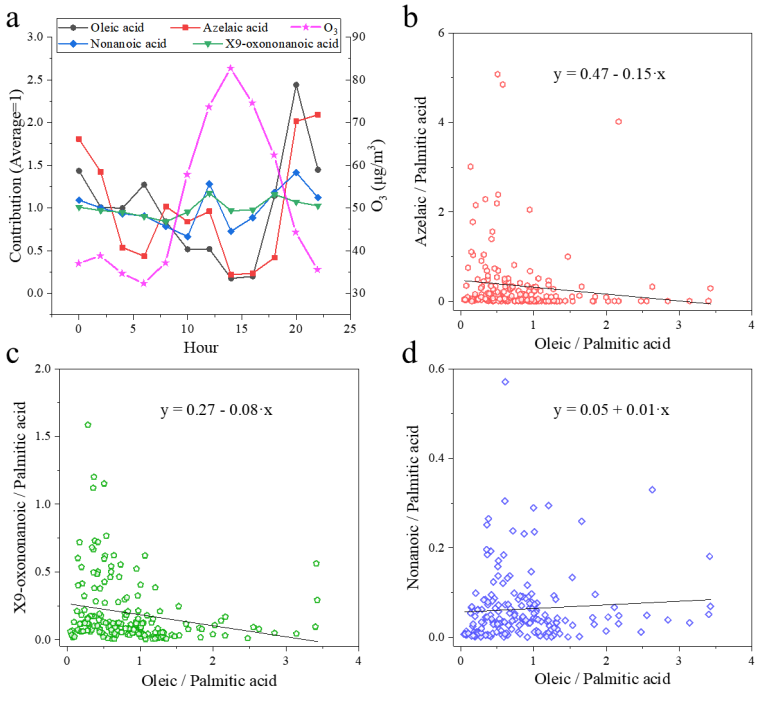

Figure 8. Correlation of C_9 product X9-Oxononanoic acid with oleic acid and diurnal variation of C_9 product and oleic acid in environmental samples compared to O_3.

Fig.9 shows the correlation between X9-oxononanoic acid/palmitic acid and oleic acid/palmitic acid in each cluster. Figure S3 shows the correlation of azelaic (nonanoic) acid /palmitic acid ratio (AA/P and NA/P) and oleic acid/palmitic acid ratio for the ambient samples. The CL#1 air mass cluster exhibits the longest range, the corresponding X9/P (AA/P, NA/P) values are relatively small among all air masses, the ODPs concentration does not correlate with Oleic acid and the low ODPs concentration is inconsistent with other literature findings of more aging aerosol production from long-range transport (Wang et al., 2020), suggesting that long-range air mass transport from the northwest is not the main

https://doi.org/10.5194/acp-2022-586
Preprint. Discussion started: 5 September 2022

Atmospheric Chemistry and Physics Discussions

source of cooking emissions in Changzhou during the observation. In CL#2 and CL#4, X9/P is larger than that in CL#1 and CL#3, and AA/P and NA/P have the same characteristics. The contribution of X9-Oxononanoic acid, etc. may come from the ozonolysis of unsaturated fatty acids as well as transport effects. In CL#3, the highest concentrations of $PM_{2.5}$, OC, NO_2, and the lowest concentrations of ozone were observed. The degradation extent of oleic acid was alleviated, resulting in a relatively low concentration of ODPs. In CL#2 and CL#4, the ratio of oleic acid to palmitic acid is relatively small while temperature and ozone concentration is higher, ozone decomposition ratio of oleic acid is larger, and C_9 productions were relatively high. A more pronounced negative correlation between X9/P and O/P is observed in CL#2 than in CL#4, suggesting that more chemical production of the ODPs in CL#2 than that in CL#4 (Figure S4). The maximum wind speed and the minimum NO_2 concentration were observed under the influence of CL#4, which carried the largest proportion of C_9 products due to the combined effects from the pollutants carried by CL#4 and the ozone decomposition of unsaturated fatty acids emitted by local cooking. TFAs and ODPs emitted by cooking in surrounding areas contribute significantly to cooking aerosol in Changzhou.

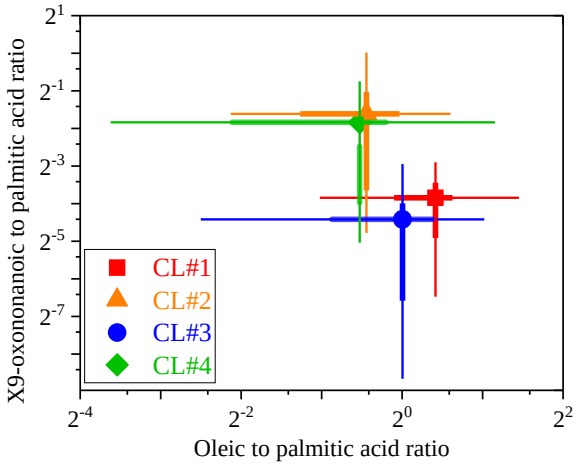

Figure 9. Correlation of X9-Oxononanoic acid/palmitic acid ratio and oleic acid/palmitic acid ratio for the ambient samples in each type of air masses (Various solid shapes represent the mean of different clusters; Thick whiskers indicate the 25th and 75th percentiles, slender whiskers are the 5th and 95th percentiles).

3.5 Oxidative decomposition of unsaturated fatty acids

From the above analysis, both sFAs and uFAs from cooking emissions reach high values between 18:00 and 22:00 pm (around dinner time), and then begin to decline until breakfast time. Fatty acid-like substances in fresh cooking emissions react with various oxidants while being continuously replenished by the fresh cooking emission during the day so that the degradation of uFAs in the particulate phase is complicated. With no obvious fresh cooking emissions after

https://doi.org/10.5194/acp-2022-586
Preprint. Discussion started: 5 September 2022


Atmospheric Chemistry and Physics Discussions

dinner, and the low volatility of the target pollutants studied (oleic and linoleic acids), the effect of gas-particle partitioning on them can be disregarded, and the evening provides a good opportunity to study the chemical degradation of uFAs from cooking emissions. Therefore, the experiment selected part of the period from 18 in the evening to 6 in the morning of the next day to conduct research, focusing on the impact of oxidants in the atmospheric environment on unsaturated fatty acids. To calculate the rate constant of uFAs with oxidants (especially O_3 and NO_3^*., etc), a one-step model was utilized, and an average decay rate constant in each night could be derived. The same method has been used in the study of Wang and Yu (2021), which shows that more than 77% of the observed data fits better with a one-step model. Figures S5 and S6 show the night-time oxidative degradation of oleic acid and linoleic acid, respectively. It should be noted that not all of the reactants (uFAs) will be fully consumed from the start of the fit until fresh emissions are added to the atmosphere, and the amount of consumed and remaining uFAs could be affected by a combination of oxidant level, source activity, and meteorological conditions.

The definition of the effective rate constant k has been described in previous studies of Donahue et al. (2005) and Wang and Yu (2021). Fig.10 shows the effective rate constants of the oxidative decomposition of oleic(k_O) and linoleic(k_L) acids in relation to air oxidants (O_3, NO_2, O_x and NO_3^*, etc.). It should be noted that the NO_3^*, which is calculated by multiplying O_3 by NO_2, is a substitution for NO_3^* radical, which is not available in this campaign. Both k_O and k_L had a significant positive correlation (The P values of significance tests were all less than 0.005) with O_3 was observed, and had a consistent trend with O_x and NO_3^*, but no correlation was observed with NO_2. Ozone acted as the predominant oxidant for the oxidative decomposition of uFAs. The difference is that the correlation between the effective rate constants of oxidative decomposition and ozone concentration was only observed for oleic and linoleic acids in Shanghai. This may be due to the higher ozone concentration and higher temperature during the observation period, which are more conducive to the oxidative reactions between uFAs and other oxidants (O_x and NO_3^*, etc.). In addition to the oxidants mentioned above, laboratory studies has also reported N_2O_5 reacts with olefinic acids containing C=C bonds such as oleic acid and linoleic acid, which has a much slower reaction kinetics than that of NO_3^* (Gross et al., 2009). So the effect of N_2O_5 was ignored in this study.

Fig.11 shows the scatter plot of the effective rate constants of oleic and linoleic acid. The significant correlation between the effective rate constants of oleic acid and linoleic acid was not equal to 1 due to the differences in aerosol composition and environmental conditions. The effective rate constant of oleic acid ranged from 0.12-0.41 h^{-1}, which was overall smaller than k_L (0.25-0.50 h^{-1}), indicating that their reactivity is closely related to their chemical structure, and the

https://doi.org/10.5194/acp-2022-586
Preprint. Discussion started: 5 September 2022

Atmospheric Chemistry and Physics Discussions

two C=C bonds in the linoleic make a higher probability in reacting with atmospheric oxidants. However, besides the chemical structure, other factors (e.g., gas-particle phase partitioning, diffusion, and temperature) also affect the calculation of oxidation reaction rate of uFAs. The fitted ratio of k_L/k_O is 1.32 (red dashed line in Fig.11), with most scatters fall in the area with k_L to k_O values above the 1:1. k_L /k_O has a mean value of 1.5 ± 0.3 and the relative reactivity of linoleic acid to oleic acid is below 2 in the measured environmental data, but close to the results of laboratory studies with O_3 as oxidant. We also reviewed the k_L/k_O ratios of O_3, NO_3^* and N_2O_5 as oxidants in other laboratory studies, and the k_L/k_O ratios of the three oxidants were 1.7, 1.8 and 2.9 (Gross et al., 2009; Thornberry and Abbatt, 2004), respectively, which are slightly higher than our results. The comparison indicates that O_3 was the most likely oxidants for the nighttime uFAs oxidation in the urban area of Changzhou.

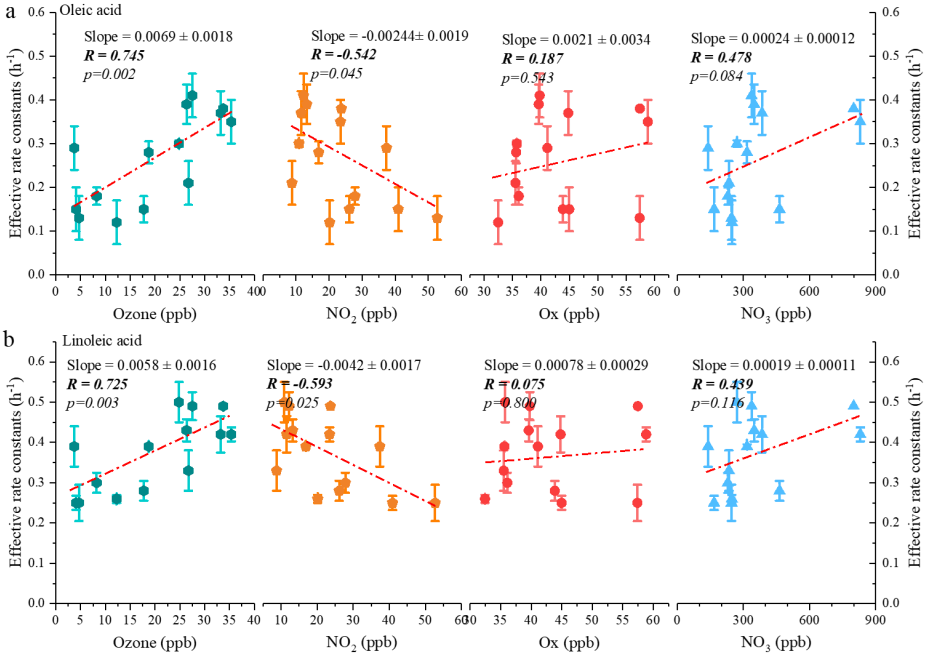

Figure 10. Correlations of the estimated effective decay rate constant with average nighttime atmospheric oxidants concentration for oleic acid (a) and linoleic acid (b).

https://doi.org/10.5194/acp-2022-586
Preprint. Discussion started: 5 September 2022

Atmospheric Chemistry and Physics Discussions

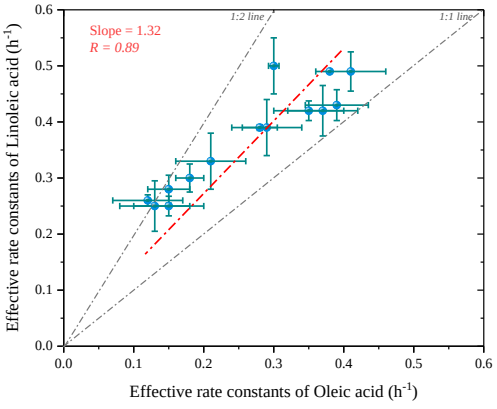

Figure 11. Scatter plots of estimated effective rate constant for oleic acid versus linoleic acid.

3.6 Source contributions of cooking aerosol to $PM_{2.5}$ and OC

To gain a more quantitative assessment of source contribution from cooking to OA, PMF was applied for source apportionment. The target POA markers were incorporated into the input data matrix, along with SOA markers (Table S1) and major aerosol components including major ions, elements, EC, and OC. A detailed source apportionment analysis utilizing the same set of organic source markers measured in this field campaign is reported in a separate paper in combination with inorganic ions and elemental species at CEMC (in pre-writing). Below we will only present PMF results related to the abovementioned POA markers. Identification of each PMF-resolved source factor is shown in section S2.

In a specific pollution period, different sources have different impacts on $PM_{2.5}$ concentration and chemical compositions in Changzhou. Among the 10 sources of $PM_{2.5}$ analyzed by the PMF model, the cooking factor was dominated by sFAs and uFAs during the monitoring period, accounting for 4.8% of the total $PM_{2.5}$ (Li et al., 2020). Cooking source also showed a clear diurnal variation, with two peaks at around 6:00 and 20:00 local, respectively, especially at the dinner time. The contribution of cooking to $PM_{2.5}$ concentration during meal time increased significantly compared with other periods, reaching 6.1% at dinner time, and the fatty acid concentration as cooking tracers increased significantly during dinner time compared with afternoon. The mean concentration of cooking aerosol in the polluted period was estimated to be 3.63 $\mu g/m^3$, which was 3.9 times higher than that in the clean period (0.90 $\mu g/m^3$), and similar to the variation of fatty acid. Overall, we estimated that cooking accounted for 5.6% of the total $PM_{2.5}$ during the pollution period, which was 1.8 times greater than that of 3.2% at the clean period. Consistent with the conclusions in Section 3.3, the mass concentration of $PM_{2.5}$ and OC were significantly influenced by emission sources. During the

https://doi.org/10.5194/acp-2022-586
Preprint. Discussion started: 5 September 2022

Atmospheric Chemistry and Physics Discussions

whole observation period, the cooking factor contributes only a small percent of $PM_{2.5}$ (4%, Figure S7), but it accounts for 10.8% of the total OC, indicating the importance of cooking emissions to organic matter, a significant source of organic pollution in urban areas.

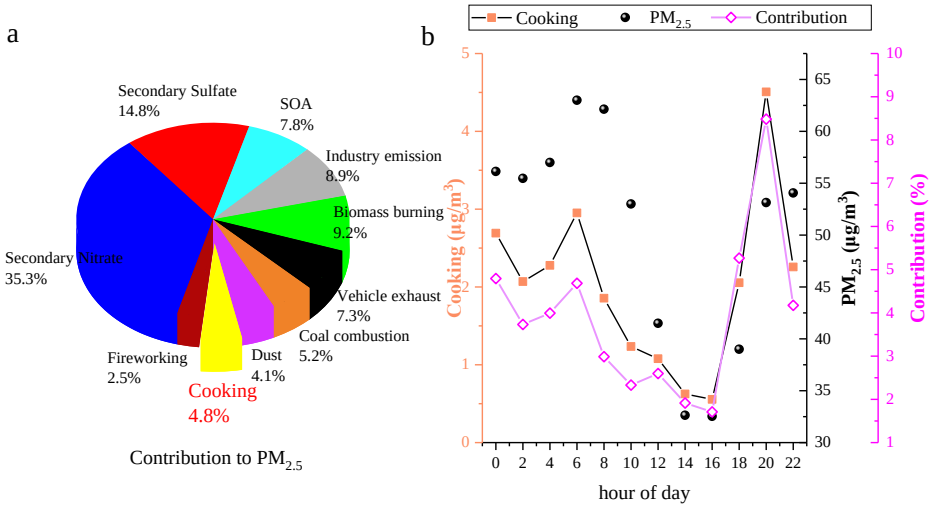

Figure 12. Comparison of individual factor contributions to $PM_{2.5}$ (a); diurnal variation of cooking source (b).

4. Conclusions

In this study, we measured uFAs, sFAs, and ODPs every two hours using TAG in the Changzhou city. The concentration of TFAs averaged at 105.70 ng/m^3, which is close to the concentrations in Shanghai. The average concentration of total TFAs in polluted period was 147.06 ng/m^3, which was 4.2 times higher than that in clean period, higher than the ratio of $PM_{2.5}$ and OC concentrations in polluted hours to clean hours. During the rising period of $PM_{2.5}$, TFAs concentration tends to reach the concentration peak earlier than $PM_{2.5}$, and the proportion of TFAs in $PM_{2.5}$ as well as OC will increase first and then decrease. However, when affected by adverse diffusion, TFAs concentration will accumulate continuously as $PM_{2.5}$.

Fatty acids concentration showed a clear diurnal variation, with high values in the morning (6:00 am) and evening (20:00 pm), especially around dinner time. The average contribution of cooking factor to $PM_{2.5}$ concentration was estimated to be 4.8%, while the contribution to total OC may reach 10.8%. However, the proportion of cooking among different sources during the meal period increased significantly compared with other periods, especially the dinner period, peaking at 6.1%. Linoleic acid /Palmitic acid and Oleic acid /Palmitic acid values were significantly higher at dinning time, more pronounced at dinner than lunchtime, and closer to the source profile values measured directly at the source.

https://doi.org/10.5194/acp-2022-586
Preprint. Discussion started: 5 September 2022

Atmospheric Chemistry and Physics Discussions

Diurnal trend of ODPs is different from that of uFAs, and the concentration of ODPs increased significantly at noon. The diurnal variations of nonanoic acid and X9-oxononanoic acid in ODPs are relatively similar, mainly because oleic acid can produce both X9-oxononanoic acid and nonanoic acid in the ozonolysis pathway.

Under the influence of air masses from different directions, there were significant differences in the ratios of various organic acids from cooking. The highest total concentrations of sFAs, uFAs and ODPs were found under CL#3. At the influence of CL#2 and CL#4 air masses, the oxidative decomposition activities of unsaturated fatty acids emitted from local culinary sources were more active, with a more significant negative correlation between X9/P and O/P, suggesting that more ODPs come from the oxidative decomposition of acids emitted from local cooking under the influence of the CL#2 and CL#4. The daily oxidative degradation kinetics of oleic and linoleic acids were obtained using data during nighttime of each observation date. The k_O ranged from 0.12 to 0.41 h^{-1}, which was overall smaller than k_L (0.25-0.50 h^{-1}). It was observed that both k_O and k_L had a significant positive correlation with O_3, and had a consistent trend with O_x and NO_3^*. The relative reaction coefficients k_L/k_O (1.5 ±0.3) of oleic and linoleic acids in this paper are close to k_L/k_O measured for O_3 and NO_3^* in laboratory studies, indicating that O_3 and NO_3^* are the main nighttime oxidants for uFAs in Changzhou City. Overall, this study describes the concentration variation and oxidative degradation of fatty acids and oxidation products in ambient air based on hourly time-resolved observations, guiding future refinement of source apportionment of $PM_{2.5}$ and the development of cooking emission control policies. The contribution of cooking aerosol to $PM_{2.5}$ is 4.8% on average, rising to 6.1% at dinner time, and the fatty acid concentration as cooking tracers increased significantly during dinner time compared with afternoon. It is estimated that cooking source accounted for 5.6% of the total $PM_{2.5}$ during the pollution period, which was 1.8 times greater than that of 3.2% at the clean period, showing that strict control on cooking emissions should be paid more attention during pollution episodes.

ACKNOWLEDGEMENTS

This study is financially supported by the National Natural Science Foundation of China (NO. 41875161, 42075144 and 42005112).

AUTHOR CONTRIBUTIONS

LL formulated the research goals and edited and reviewed the manuscript. QL, KZ, RL and LMY conducted the field measurements. QL and KZ performed the data analysis and prepared the manuscript with contributions from all co-authors. LL and JZY reviewed and edited the manuscript. All authors contributed to data interpretations and discussions.

https://doi.org/10.5194/acp-2022-586
Preprint. Discussion started: 5 September 2022

Atmospheric Chemistry and Physics Discussions

COMPETING INTERESTS

The authors declare no conflict of interest.

DATA AND CODE AVAILABILITY

This paper does not report original code. Data is available from the corresponding author (Lily@shu.edu.cn) upon request.

REFERENCES

Amato, F., Pandolfi, M., Escrig, A., Querol, X., Alastuey, A., Pey, J., Perez, N., and Hopke, P. K.: Quantifying road dust resuspension in urban environment by Multilinear Engine: A comparison with PMF2, Atmos. Environ., 43(17), 2770-2780, doi:10.1016/j.atmosenv.2009.02.039, 2009.

An, Z. J., Ren, H. X., Xue, M., Guan, X. S., and Jiang, J. K.: Comprehensive two-dimensional gas chromatography mass spectrometry with a solid-state thermal modulator for in-situ speciated measurement of organic aerosols, J. Chromatogr. A, 1625, doi: 10.1016/j.chroma.2020.461336, 2020.

Bertrand, A., Stefenelli, G., Jen, C. N., Pieber, S. M., Bruns, E. A., Ni, H. Y., Temime-Roussel, B., Slowik, J. G., Goldstein, A. H., El Haddad, I., Baltensperger, U., Prevot, A. S. H., Wortham, H., and Marchand, N.: Evolution of the chemical fingerprint of biomass burning organic aerosol during aging, Atmos. Chem. Phys., 18(10), 7607-7624, doi:10.5194/acp-18-7607-2018, 2018a.

Bertrand, A., Stefenelli, G., Pieber, S. M., Bruns, E. A., Temime-Roussel, B., Slowik, J. G., Wortham, H., Prevot, A. S. H., El Haddad, I., and Marchand, N.: Influence of the vapor wall loss on the degradation rate constants in chamber experiments of levoglucosan and other biomass burning markers, Atmos. Chem. Phys., 18(15), 10915-10930, doi:10.5194/acp-18-10915-2018, 2018b.

Donahue, N. M., Robinson, A. L., Huff Hartz, K. E., Sage, A. M., and Weitkamp, E. A.: Competitive oxidation in atmospheric aerosols: The case for relative kinetics, Geophys. Res. Lett., 32(16), doi: 10.1029/2005gl022893, 2005.

Fortenberry, C., Walker, M., Dang, A., Loka, A., Date, G., de Caryalho, K. C., Morrison, G., and Williams, B.: Analysis of indoor particles and gases and their evolution with natural ventilation, Indoor Air, 29(5), 761-779, doi:10.1111/ina.12584, 2019.

Gross, S., Iannone, R., Xiao, S., and Bertram, A. K.: Reactive uptake studies of NO_3 and N_2O_5 on alkenoic acid, alkanoate, and polyalcohol substrates to probe nighttime aerosol chemistry, Phys. Chem. Chem. Phys., 11(36), 7792-7803, doi:10.1039/b904741g, 2009.

Guo, J., Rahn, K. A., and Zhuang, G. S.: A mechanism for the increase of pollution elements in dust storms in Beijing, Atmos. Environ., 38(6), 855-862, doi:10.1016/j.atmosenv.2003.10.037, 2004.

He, L. Y., Hu, M., Huang, X. F., Yu, B. D., Zhang, Y. H., and Liu, D. Q.: Measurement of emissions of fine particulate organic matter from Chinese cooking, Atmos. Environ., 38(38), 6557-6564, doi:10.1016/j.atmosenv.2004.08.034, 2004.

Hou, X. M., Zhuang, G. S., Sun, Y., and An, Z. S.: Characteristics and sources of polycyclic aromatic hydrocarbons and fatty acids in $PM_{2.5}$ aerosols in dust season in China, Atmos. Environ., 40(18), 3251-3262, doi:10.1016/j.atmosenv.2006.02.003, 2006.

Huang, D. D., Zhu, S. H., An, J. Y., Wang, Q. Q., Qiao, L. P., Zhou, M., He, X., Ma, Y. G., Sun, Y. L., Huang, C., Yu, J. Z., and Zhang, Q.: Comparative assessment of cooking emission contributions to urban organic aerosol using nnline molecular tracers and aerosol mass spectrometry measurements, Environ. Sci. Technol., 55(21), 14526-14535,

485 doi:10.1021/acs.est.1c03280, 2021.
486 Huang, X. Q., Han, D. M., Cheng, J. P., Chen, X. J., Zhou, Y., Liao, H. X., Dong, W., and Yuan, C.: Characteristics
487 and health risk assessment of volatile organic compounds (VOCs) in restaurants in Shanghai, Environ. Sci. Pollut. R.,
488 27(1), 490-499, doi:10.1007/s11356-019-06881-6, 2020.
489 Huff, H. B., Krivonos, E., and van der Mensbrugghe, D.: Review and synthesis of empirical results of studies of
490 world trade organization agricultural trade reform, Reforming Agricultural Trade for Developing Countries, Vol 2, 20-39,
491 2007.
492 Kanakidou, M., Seinfeld, J. H., Pandis, S. N., Barnes, I., Dentener, F. J., Facchini, M. C., Van Dingenen, R., Ervens,
493 B., Nenes, A., Nielsen, C. J., Swietlicki, E., Putaud, J. P., Balkanski, Y., Fuzzi, S., Horth, J., Moortgat, G. K., Winterhalter,
494 R., Myhre, C. E. L., Tsigaridis, K., Vignati, E., Stephanou, E. G., and Wilson, J.: Organic aerosol and global climate
495 modelling: a review, Atmos. Chem. Phys., 5, 1053-1123, doi:DOI 10.5194/acp-5-1053-2005, 2005.
496 Lee, S., Liu, W., Wang, Y. H., Russell, A. G., and Edgerton, E. S.: Source apportionment of $PM_{2.5}$: Comparing PMF
497 and CMB results for four ambient monitoriniz sites in the southeastern United States, Atmos. Environ., 42(18), 4126-
498 4137, doi:10.1016/j.atmosenv.2008.01.025, 2008.
499 Li, L., Wu, D., Chang, X., Tang, Y., Hua, Y., Xu, Q. C., Deng, S. H., Wang, S. X., and Hao, J. M.: Polar organic
500 aerosol tracers in two areas in Beijing-Tianjin-Hebei region: Concentration comparison before and in the sept. Third
501 Parade and sources, Environ. Pollut., 270, doi: 10.1016/j.envpol.2020.116108, 2021.
502 Li, R., Wang, Q. Q., He, X., Zhu, S. H., Zhang, K., Duan, Y. S., Fu, Q. Y., Qiao, L. P., Wang, Y. J., Huang, L., Li, L.,
503 and Yu, J. Z.: Source apportionment of $PM_{2.5}$ in Shanghai based on hourly organic molecular markers and other source
504 tracers, Atmos. Chem. Phys., 20(20), 12047-12061, doi:10.5194/acp-20-12047-2020, 2020.
505 Nah, T., Kessler, S. H., Daumit, K. E., Kroll, J. H., Leone, S. R., and Wilson, K. R.: Influence of molecular structure
506 and chemical functionality on the heterogeneous OH-initiated oxidation of unsaturated organic particles, J. Phys. Chem.
507 A, 118(23), 4106-4119, doi:10.1021/jp502666g, 2014.
508 Norris, G., Duvall, R., Brown, S., and Bai, S.: EPA positive matrix factorization (PMF) 5.0 fundamentals and user
509 guide, U.S. Environmental Protection Agency, Washington, DC, EPA/600/R-14/108 (NTIS PB2015-105147), 2014.
510 Pei, B., Cui, H. Y., Liu, H., and Yan, N. Q.: Chemical characteristics of fine particulate matter emitted from
511 commercial cooking, Front. Env. Sci. Eng., 10(3), 559-568, doi:10.1007/s11783-016-0829-y, 2016.
512 Pleik, S., Spengler, B., Schafer, T., Urbach, D., Luhn, S., and Kirsch, D.: Fatty acid structure and degradation
513 analysis in fingerprint residues, J. Am. Soc. Mass. Spectrom., 27(9), 1565-1574, doi:10.1007/s13361-016-1429-6, 2016.
514 Ren, H. X., Xue, M., An, Z. J., Zhou, W., and Jiang, J. K.: Quartz filter-based thermal desorption gas
515 chromatography mass spectrometry for in-situ molecular level measurement of ambient organic aerosols, J. Chromatogr.
516 A, 1589, 141-148, doi:10.1016/j.chroma.2019.01.010, 2019.
517 Ringuet, J., Leoz-Garziandia, E., Budzinski, H., Villenave, E., and Albinet, A.: Particle size distribution of nitrated
518 and oxygenated polycyclic aromatic hydrocarbons (NPAHs and OPAHs) on traffic and suburban sites of a European
519 megacity: Paris (France), Atmos. Chem. Phys., 12(18), 8877-8887, doi:10.5194/acp-12-8877-2012, 2012.
520 Schauer, C., Niessner, R., and Poschl, U.: Polycyclic aromatic hydrocarbons in urban air particulate matter: Decadal
521 and seasonal trends, chemical degradation, and sampling artifacts, Environ. Sci. Technol., 37(13), 2861-2868,
522 doi:10.1021/es034059s, 2003.
523 Schauer, J. J., Kleeman, M. J., Cass, G. R., and Simoneit, B. R. T.: Measurement of emissions from air pollution
524 sources. 4. C-1-C-27 organic compounds from cooking with seed oils, Environ. Sci. Technol., 36(4), 567-575,
525 doi:10.1021/es002053m, 2002.
526 Thornberry, T., and Abbatt, J. P. D.: Heterogeneous reaction of ozone with liquid unsaturated fatty acids: detailed

https://doi.org/10.5194/acp-2022-586
Preprint. Discussion started: 5 September 2022

Atmospheric Chemistry and Physics Discussions

kinetics and gas-phase product studies, Phys. Chem. Chem. Phys., 6(1), 84-93, doi:10.1039/b310149e, 2004.

Vesna, O., Sax, M., Kalberer, M., Gaschen, A., and Ammann, M.: Product study of oleic acid ozonolysis as function of humidity, Atmos. Environ., 43(24), 3662-3669, doi:10.1016/j.atmosenv.2009.04.047, 2009.

Wang, Q. Q., He, X., Huang, X. H. H., Griffith, S. M., Feng, Y. M., Zhang, T., Zhang, Q. Y., Wu, D., and Yu, J. Z.: Impact of secondary organic aerosol tracers on tracer-based source apportionment of organic carbon and $PM_{2.5}$: A case study in the Pearl River Delta, China, Acs Earth Space Chem., 1(9), 562-571, doi:10.1021/acsearthspacechem.7b00088, 2017.

Wang, Q. Q., He, X., Zhou, M., Huang, D. D., Qiao, L. P., Zhu, S. H., Ma, Y. G., Wang, H. L., Li, L., Huang, C., Huang, X. H. H., Xu, W., Worsnop, D., Goldstein, A. H., Guo, H., and Yu, J. Z.: Hourly measurements of organic molecular markers in urban Shanghai, China: Primary organic aerosol source identification and observation of cooking aerosol aging, Acs Earth Space Chem., 4(9), 1670-1685, doi:10.1021/acsearthspacechem.0c00205, 2020.

Wang, Q. Q., and Yu, J. Z.: Ambient measurements of heterogeneous ozone oxidation rates of oleic, elaidic, and linoleic acid using a relative rate constant approach in an urban environment, Geophys. Res. Lett., 48(19), doi: 10.1029/2021GL095130, 2021.

Yee, L. D., Isaacman-VanWertz, G., Wernis, R. A., Meng, M., Rivera, V., Kreisberg, N. M., Hering, S. V., Bering, M. S., Glasius, M., Upshur, M. A., Be, A. G., Thomson, R. J., Geiger, F. M., Offenberg, J. H., Lewandowski, M., Kourtchev, I., Kalberer, M., de Sa, S., Martin, S. T., Alexander, M. L., Palm, B. B., Hu, W. W., Campuzano-Jost, P., Day, D. A., Jimenez, J. L., Liu, Y. J., McKinney, K. A., Artaxo, P., Viegas, J., Manzi, A., Oliveira, M. B., de Souza, R., Machado, L. A. T., Longo, K., and Goldstein, A. H.: Observations of sesquiterpenes and their oxidation products in central Amazonia during the wet and dry seasons, Atmos. Chem. Phys., 18(14), 10433-10457, doi:10.5194/acp-18-10433-2018, 2018.

Zahardis, J., and Petrucci, G. A.: The oleic acid-ozone heterogeneous reaction system: products, kinetics, secondary chemistry, and atmospheric implications of a model system - a review, Atmos. Chem. Phys., 7, 1237-1274, doi:DOI 10.5194/acp-7-1237-2007, 2007.

Zhang, K., Yang, L. M., Li, Q., Li, R., Zhang, D. P., Xu, W., Feng, J. L., Wang, Q. Q., Wang, W., Huang, L., Yaluk, E. A., Wang, Y. J., Yu, J. Z., and Li, L.: Hourly measurement of $PM_{2.5}$-bound nonpolar organic compounds in Shanghai: Characteristics, sources and health risk assessment, Sci. Total Environ., 789, doi: 10.1016/j.scitotenv.2021.148070, 2021.

Zhang, N., Han, B., He, F., Xu, J., Zhao, R. J., Zhang, Y. J., and Bai, Z. P.: Chemical characteristic of $PM_{2.5}$ emission and inhalational carcinogenic risk of domestic Chinese cooking, Environ. Pollut., 227, 24-30, doi:10.1016/j.envpol.2017.04.033, 2017.

Zhao, Y. L., Hu, M., Slanina, S., and Zhang, Y. H.: Chemical compositions of fine particulate organic matter emitted from Chinese cooking, Environ. Sci. Technol., 41(1), 99-105, doi:10.1021/es0614518, 2007.

Ziemann, P. J.: Aerosol products, mechanisms, and kinetics of heterogeneous reactions of ozone with oleic acid in pure and mixed particles, Faraday Discuss., 130, 469-490, 2005.